Middle Pennsylvanian composite stratigraphic section of Holman Grade records cyclic fluvio-δic sedimentation within the Taos trough axis

D. E. Sweet and A. J. Watters

2015, pp. 229-239. https://doi.org/10.56577/FFC-66.229

in:

Guidebook 66 - Geology of the Las Vegas Area, Lindline, Jennifer; Petronis, Michael; Zebrowski, Joseph, New Mexico Geological Society 66th Annual Fall Field Conference Guidebook, 312 p. https://doi.org/10.56577/FFC-66

This page is intentionally left blank to maintain order of facing pages.

MIDDLE PENNSYLVANIAN COMPOSITE STRATIGRAPHIC SECTION OF HOLMAN GRADE RECORDS CYCLIC FLUVIO-DELTAIC SEDIMENTATION WITHIN THE TAOS TROUGH AXIS

D. E. SWEET[1] AND A. J. WATTERS[2]
[1] Department of Geosciences, Texas Tech University, Lubbock, TX, dustin.sweet@ttu.edu
[2] ConocoPhillips, 600 North Dairy Ashford Road, Houston, TX

ABSTRACT—The Taos trough is a structurally-controlled basin formed from stresses related to the ancestral Rocky Mountain orogeny. Pennsylvanian sediments derived locally from Precambrian-cored uplifts fill the basin. However, structural models proposed for the development of the basin conflict. One model proposes flexure from emplacement of crustal load via a thrust fault to the west of the basin. The other model invokes intrabasinal strain manifested in thrusts with Precambrian-cored hanging walls and a strike-slip bounding fault to the west.

To test these competing models, we have accumulated detailed sedimentologic and stratigraphic data from a location within the axis of the Taos trough. Specifically, we construct a detailed composite stratigraphic column for the Holman grade area using a series of road cuts along Highway 518. Construction of the column accounts for along strike duplication of strata, covered section and broad folding in the area. The composite section is ~950 m thick and is primarily composed of shallowing upward cycles that grade upward from offshore marine mudstone to a cycle cap of lower shoreface facies, upper shoreface facies, or nonmarine facies. These cycles are best characterized as fluvio-deltaic cycles. The persistent occurrence of shallow marine and nonmarine facies at the base of the section are difficult to reconcile with a flexural basin model, which often predicts a long-term, gradual shallowing as flexural accommodation that is progressively filled. Our analysis appears to show the opposite trend, albeit inconclusive, as the interval studied does not represent the entire section.

INTRODUCTION

The Taos trough is one of numerous depocenters that record late Paleozoic intracontinental deformation known as the ancestral Rocky Mountains (Fig. 1; e.g., Kluth and Coney, 1981). Subsequent uplift, related to Laramide shortening, has exhumed the core of the Taos trough within the Sangre de Cristo Mountains of northern New Mexico (e.g., Yin and Ingersoll, 1997). Northwest of Mora, New Mexico, lower to middle Pennsylvanian strata records the filling of the Taos trough axis (Soegaard, 1990; Baltz and Myers, 1999). However, different structural basin models have been proposed for the Taos trough. For example, Soegaard (1990) considered the Taos trough as a north-south trending, west-loaded, flexural basin where sediment was sourced primarily from Precambrian rocks to the west. In contrast, Baltz and Myers (1999) suggest that sedimentary dispersal patterns and depocenters of the Taos trough region were also influenced by intrabasinal, Precambrian-cored uplifts.

These two competing basin models predict different styles of basin fill. For example, a basin undergoing load emplacement flexure contains a foredeep that is progressively filled, thus the sedimentary package should shallow upward over the history of the basin (e.g., DeCelles and Giles, 1996; Barbeau, 2003). In the Soegaard (1990) flexural model for the Taos trough, the axis is portrayed as the underfilled foredeep that was filled with fans from the west. However, in the Baltz and Myers (1999) basin model, the Taos trough axis is likely fed with sediments from both the west and the east and allows for much shallower deposition throughout the basin fill history.

To gather data to test these two competing models, we have constructed a detailed composite stratigraphic column using road cuts along the Holman grade of Highway 518. The purpose of this paper is to detail the construction process used to assemble the composite with accompanying facies analysis. Our results suggest that approximately 950 m of stratigraphic section exists along Holman Grade and the total takes into account laterally equivalent strata and covered intervals. Moreover, strata in the lower 490 m of the section contain non-marine facies.

STRATIGRAPHY AND TECTONIC ELEMENTS OF THE TAOS TROUGH

In northern New Mexico, the tectonic elements of the ancestral Rocky Mountains consist of the Taos trough bounded by Precambrian uplifts to the west and east, the southern Uncompahgre uplift, and the Sierra Grande uplift, respectively (Fig. 1). In many ancestral Rocky Mountains paleogeographic maps, the Taos trough connects northward with the Central Colorado trough (e.g. Kluth and Coney, 1981; Lindsey et al., 1986; Hoy and Ridgway, 2002; Sweet and Soreghan, 2010). Baltz and Myers (1999) hypothesized that the Cimarron arch was a positive region that separated the Central Colorado trough from the Taos trough based on comparing isopach trends of Pennsylvanian and Lower Permian strata and presence of thin Permian and Triassic strata atop the region.

The stratigraphic nomenclature and subsequent correlation has been an evolving process within Late Paleozoic strata of the region, however Figure 2 depicts a recent assessment. Two regional unconformities at the base of the Pennsylvanian and Permian divide the stratigraphy into three broad packages: Mississippian Tererro Formation, Pennsylvanian Sandia, Porvenir and Alamitos Formations, and Permian Sangre de Cristo and Yeso Formations. Mississippian strata are unrelated to this project other than the planar erosional surface atop the strata that suggests the area was a low relief surface prior to Pennsylvanian deformation (Baltz and Myers, 1999). Pennsylvanian strata are a mixture of shallow and deltaic marine and nearshore fluvial sediments, whereas Lower Permian strata (i.e. Sangre de Cristo

Formation) are primarily nonmarine (Sutherland, 1963; Soegaard, 1990; Baltz and Myers, 1999).

COMPOSITE STRATIGRAPHIC COLUMN CONSTRUCTION METHODS

Road cut exposures were measured with Brunton compass and Jacob staff from the base to the top of Holman Grade (Fig. 3). Each road cut along Highway 518 from the base of Holman Grade up to approximately 6.3 miles (10.1 km) where the grade flattens and the rivers drain west was treated as an individual measured section and assigned nomenclature that relates to the distance up Holman Grade from the junction of Highway 518 and Highway 121. For example, HG-1.2 refers to the measured section associated with the road cut located 1.2 miles (1.9 km) from the Highway 518 and Highway 121 junction. The thickness of covered intervals between individual sections that exhibited similar bedding orientations was geometrically calculated or measured with Jacob staff. Individual measured sections that could be correlated with confidence either due to proximity and/or lack of structure were combined into the stratigraphic sections I, II, III, IV, V, and FS723 (along Forest Service Road 723; Figs. 3, 4). These combined stratigraphic sections were compiled into the composite column through correlation of distinct stratigraphic intervals or beds coupled with sight or map projection (Fig. 4). This composite column accounts for duplication from along-strike road cuts or broad folding, as well as covered intervals.

FACIES ASSOCIATIONS AND DEPOSITIONAL CYCLICITY

The composite stratigraphic column is approximately 950 m thick and is composed of both non-marine and marine facies associations (Figs. 5, 6). These facies were originally described and interpreted in detail in Watters (2014). We summarize his analysis in Table 1. Lithologically, the Holman Grade composite section is similar to the Morrowan and Atokan Sandia Formation succession reported from the Mora River Area to the southwest (Baltz and Myers, 1984). However, Desmoinesian conodonts recovered from the base and top of the composite section are equivalent to forms found in the Porvenir Formation to the south (J.E. Barrick, personal commun., 2014). For this study, we make no lithostratigraphic correlation of the composite section, but instead focus on the entirely Desmoinesian age of the interval.

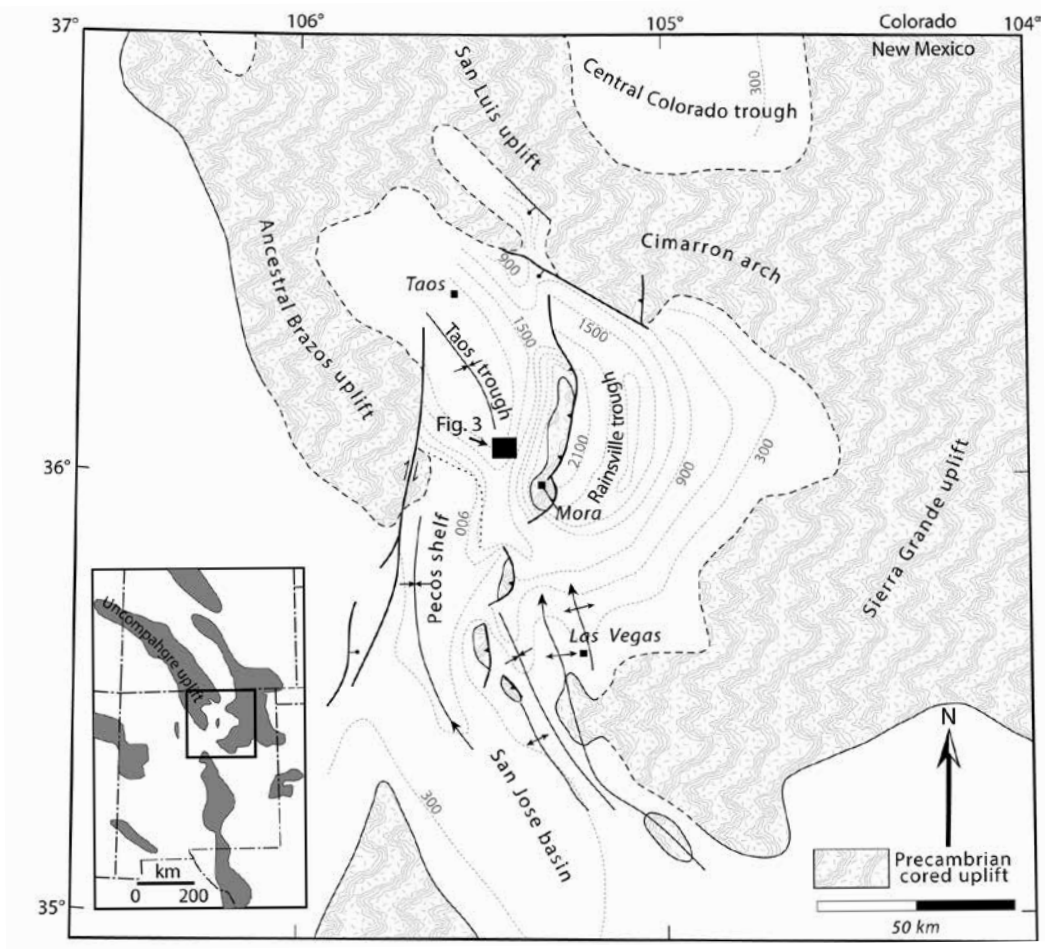

FIGURE 1.Tectonic elements of northern New Mexico. Gray dashed lines are Pennsylvanian isospachs (300 m contour interval) derived from well and outcrop data. Adapted from Baltz and Myers (1999). Black box is field area and location of Figure 3. Bottom left inset: Location of Precambrian-cored uplifts of the ancestral Rocky Mountains. Adapted from Sweet and Soreghan (2010). Note in this portrayal, the Cimarron arch does not separate the Central Colorado trough from the Taos trough region.

Facies Associations

The lower portion of the composite section contains stratigraphically-stacked facies consisting of channel–form, cross-bedded sandstone that scour into thin coaly layers and are overlain by brownish mudstone with inferred root casts that suggest nonmarine affinity for these facies (Fig. 7A). The nonmarine facies association represents approximately 3% of the facies exposed in the composite section.

The most abundant facies of the composite section are marine, consisting of sandstone, mudstone and minor amounts of carbonate. They represent >96% of the overall exposures, with the upper 670 m of the section being entirely marine. The presence of marine sedimentary structures and fossils confirm inclusion within the marine facies association. These facies can be apportioned among three associations: (1) foreshore/upper shoreface (Fig. 7B, 7C); (2) lower shoreface (Fig. 7D); and (3) offshore.

Foreshore and upper shoreface facies are defined here as those facies that occur in the marine realm but above fair-weather base (Walker, 1984; Reading, 1986). They are closely linked with the subjacent non-marine facies described above. Overall, this facies association is contained mainly within the lower 500 m of the section and represents approximately 6% of the facies exposed in the overall section.

Lower shoreface deposits are inferred in this study as those deposits that reside above storm-wave base, but below fair-weather base (Walker, 1984). The composite section contains stratigraphically-juxtaposed facies consisting of sharp-based sandstone and sandy siltstone that locally contain fossil material, most commonly plant and brachiopod fragments, and bioturbation. This association gradually increases in sand content upward into the overlying upper shoreface association. These observations coupled with the presence of hummocky cross-stratified beds indicate a lower shoreface interpretation and represents approximately 6% of the overall section exposed.

The majority of the composite section contains calcareous mudstones with fossils and plant fragments that are interbedded with thin micrite and sharp-based sandstone. This interbedded sandstone also contains plant and fossil fragments as well as load casts. This association most commonly sits stratigraphically below the lower shoreface described above, but mudstone assigned to this association also intercalate with the lower shoreface facies described above. Moreover, characteristics that indicate storm-wave base interaction are absent, thus the

TABLE 1. Facies description and interpretation.

	Facies Name	Key Characteristics	Interpretation
Nonmarine facies association	nonmarine mudstone	Weakly bedded, locally oxidized, rare plant fragments, downward bifurcating reduced zones.	Vegetated flood plain facies
	nonmarine massive sandstone	Brown to reddish tan, coarse-grained, locally oxidized, exhibits stringers of mud, vertically and laterally adjacent to nonmarine mudstone facies.	Overbank sand deposits
	carbonaceous	Brown to black, friable, with abundant (>50%) carbonaceous material, including leaf macerations and woody material. Abundant palynomorphs demonstrating high rank. Close association with nonmarine mudstone and nonmarine massive sandstone facies.	Peat to lignite coal
	cross-bedded sandstone	Reddish tan, medium-to-coarse grained, planar and trough cross-stratification. Lenticular channel-form sand bodies. Overlies and often scours into carbonaceous and nonmarine mudstone facies.	Fluvial channel fill
Foreshore/Upper Shoreface association	massive sandstone	Coarse-grained sandstone with uniform bed thickness and sharp basal contacts. Massively bedded. Lacks abundant interstitial clay. Associated with low-angle planar laminated sandstone facies.	Upper shoreface to foreshore
	Low-angle planar laminated sandstone	Moderate, fine-to-medium grained sandstone. Low-angle (<16.5°), unidirectional dipping foresets with foreset height equivalent to bed thickness.	Upper shoreface to foreshore
	trough cross-stratified sandstone	Medium to very coarse grained sandstone with up to 50% reworked carbonate fossils dispersed within siliciclastic sand. Multidirectional cosets of trough cross-bedding.	Upper shoreface
	shallow marine carbonate	Fossiliferous packstone to wackestone with variable siliciclastic component, >20 % in some wackestone	Shoreface
Lower Shoreface facies association	planar laminated sandstone	Fine-to-medium grained sandstone with well-developed planar laminations. Occasionally, rippled beds tops. Sharp basal contacts with load casts. Association with hummocky cross-stratified sandstone facies.	Lower shoreface--storm bed
	hummocky cross-stratified sandstone	Fine-to-coarse grained, fossiliferous sandstone exhibiting hummocky cross-stratification. Fossils are most commonly broken.	Lower shoreface--storm bed
Offshore facies association	offshore mudstone	Black to dark gray mudstone. Micaceous and thinly laminated shale to siltstone. Local well preserved plant fragments and fossils.	Offshore hemi-pelagic mud and distal gravity flows
	offshore laminate to massive sandstone	Very fine-to-coarse grained sandstone. Well-laminated to massive with sharp bases and local load structures. Occasional rippled beds tops. Associated with offshore mudstone facies.	Offshore sediment gravity flows
	offshore carbonate mud	silty, massive-to-wavy bedded micritic limestone. Rarely contains macrofossils. Encased by offshore mudstone facies.	Offshore carbonate

association is considered below storm-wave base and termed offshore in this study. It represents approximately 83% of the facies exposed in the overall section.

Depositional Cyclicity

Observable in the composite section are a series of stacked facies associations that represent cyclic packages. These rock packages are arranged in shallowing-upwards facies associations.

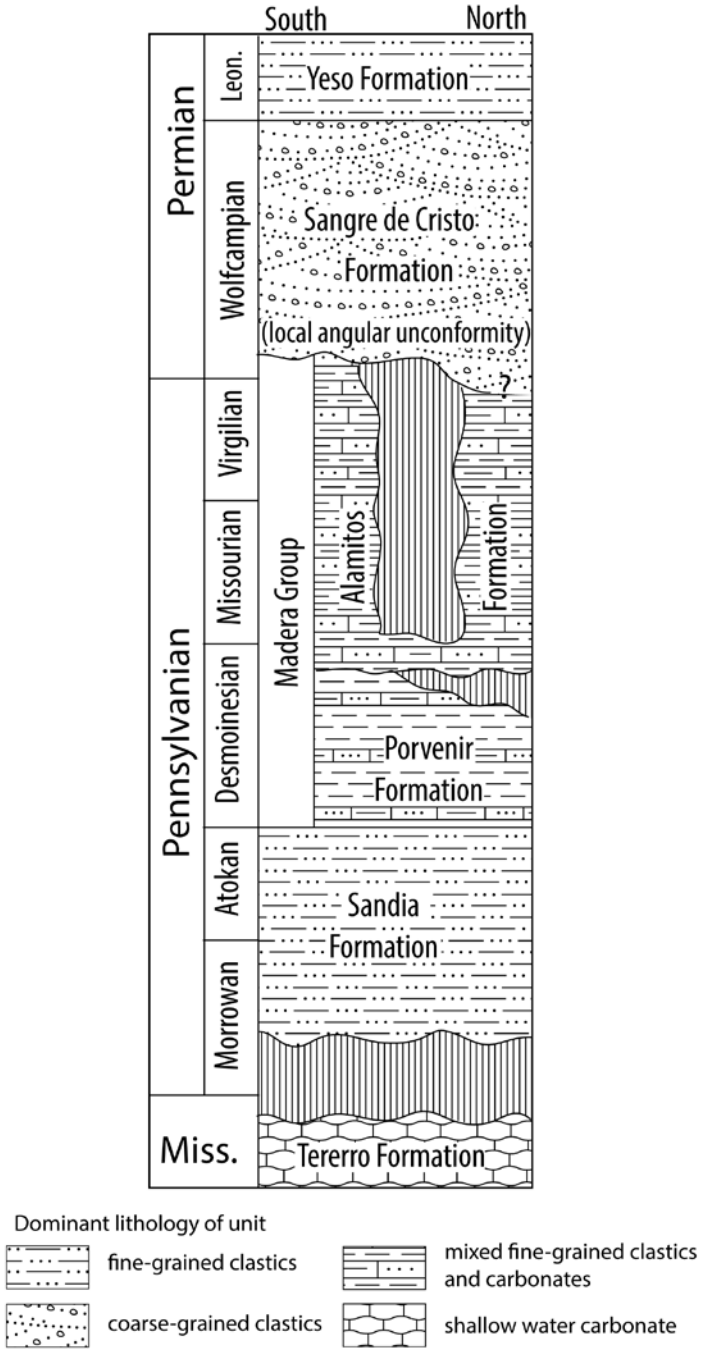

FIGURE 2. Stratigraphy, nomenclature and stratigraphic relationships in the Taos trough region. Vertical lines denote hiatuses. Adapted from Baltz and Myers (1999).

Watters (2014) noted 20 cycles in the succession and differentiated into three separate cycle types based on different cycle caps: (1) A-type cycles (either non-marine or upper shoreface/foreshore facies association top); (2) B-type cycles (lower shoreface facies association tops); and (3) C-type cycles (carbonate top).

A-type cycles are indicated by the occurrence of non-marine or foreshore/upper shoreface facies associations (Fig. 8). These are the only cycles that contain all facies associations (i.e. non-marine, foreshore/upper shoreface, lower shoreface, and offshore), but individual cycles may not contain all of the facies associations. A-type cycles occur 11 times and predominantly in the lower 300 m, but exclusively in the lower 490 m of the composite section. This cycle ranges in thickness from 10 m to 65 m.

B-type cycles are indicated by lower shoreface facies association tops that overlie offshore mudstone (Fig. 8). These cycles occur throughout the composite section and have 6 cycles exposed, which are typically thicker than A-type with the thickest cycle approximately 200 m.

C-type cycles are indicated by the occurrence of thick (>1 m) marine wackestone to grainstone carbonate as cycle tops. The tops overlie lower shoreface sandstone. The cycle occurs three times and only in the upper most 35 m of the composite section with thickness ranging from 7 m to 16 m.

Regardless of type, each cycle represents an upward shallowing of facies and thus filling accommodation space faster than it is created. For A-type cycles, the cycle base is always offshore mudstone capped by shoreface/foreshore or nonmarine facies. Internally, these cycles demonstrate the progressive upsection increase of sand, interpreted as gravity-driven, density flows in the offshore facies. These observations best characterize a fluvio-deltaic cycle (Miall, 1984). Alternatively, A-type cycles could be interpreted as non-waltherian regressive juxtaposition of facies resulting from a base level fall. For this paper, we prefer not to over interpret and assign the facies to a base level fall since the relative proportions of allogenic versus allocyclic forcing has not been determined. Moreover, the offshore mudstone is most commonly overlain by upper shoreface sandstone (Fig. 8A) which need not necessarily represent a forced regression stacking of facies.

For B-type cycles, the base is offshore mud as well, but the cycle caps are lower shoreface facies. While these are still best characterized as fluvio-deltaic cycles, they represent incomplete filling of accommodation space. Paleocurrent indicators from fluvial and foreshore strata as well as soft-sedimentary fold vergence in offshore muds indicate that sediment transport was variable, but dominantly westward (Watters, 2014) demonstrating that fluvio-deltaic lobes prograded from east-to-west.

Determining autogenic and allogenic controls on cyclicity is beyond the scope of this paper. Watters (2014) provided much discussion on this topic. Here we note that glacioeustasy likely played some part in the cyclicity since the middle Pennsylvanian cyclic strata elsewhere is widely characterized as glacio-eustatically driven (Wanless and Shepard, 1936; Veevers and Powell, 1987; Rygel et al., 2008). However, westward transport of sediment in a nearly 180° arc as demonstrated by Watters (2014) likely indicates that delta lobe switching also had a control on the cyclicity.

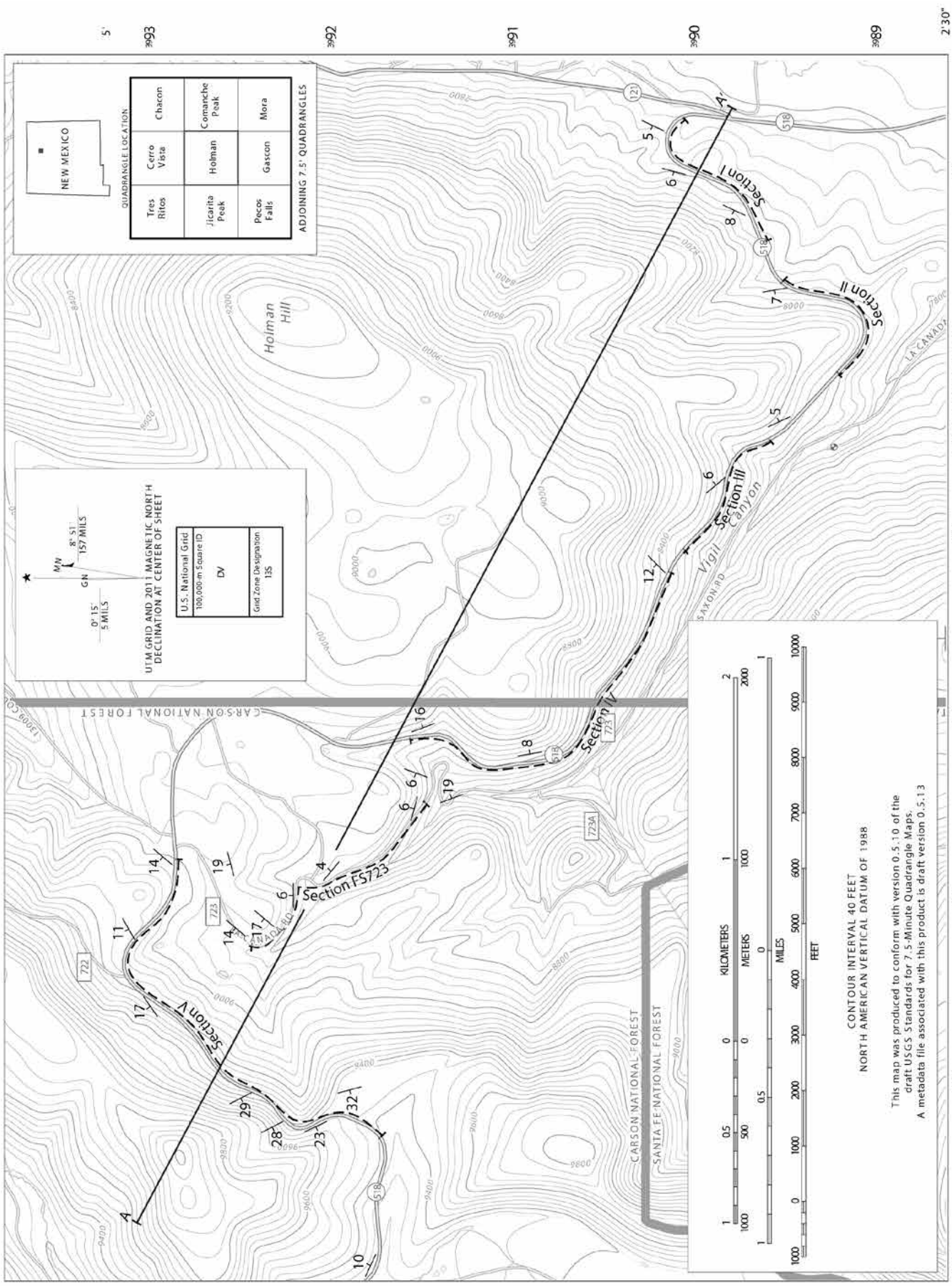

FIGURE 3. Topographic map of Holman Grade displaying the location of stratigraphic sections I, II, III, IV, V and FS723. Cross-section A-A' line is shown on Figure 4. Strike and dip of bedding is data from Pennsylvanian strata only.

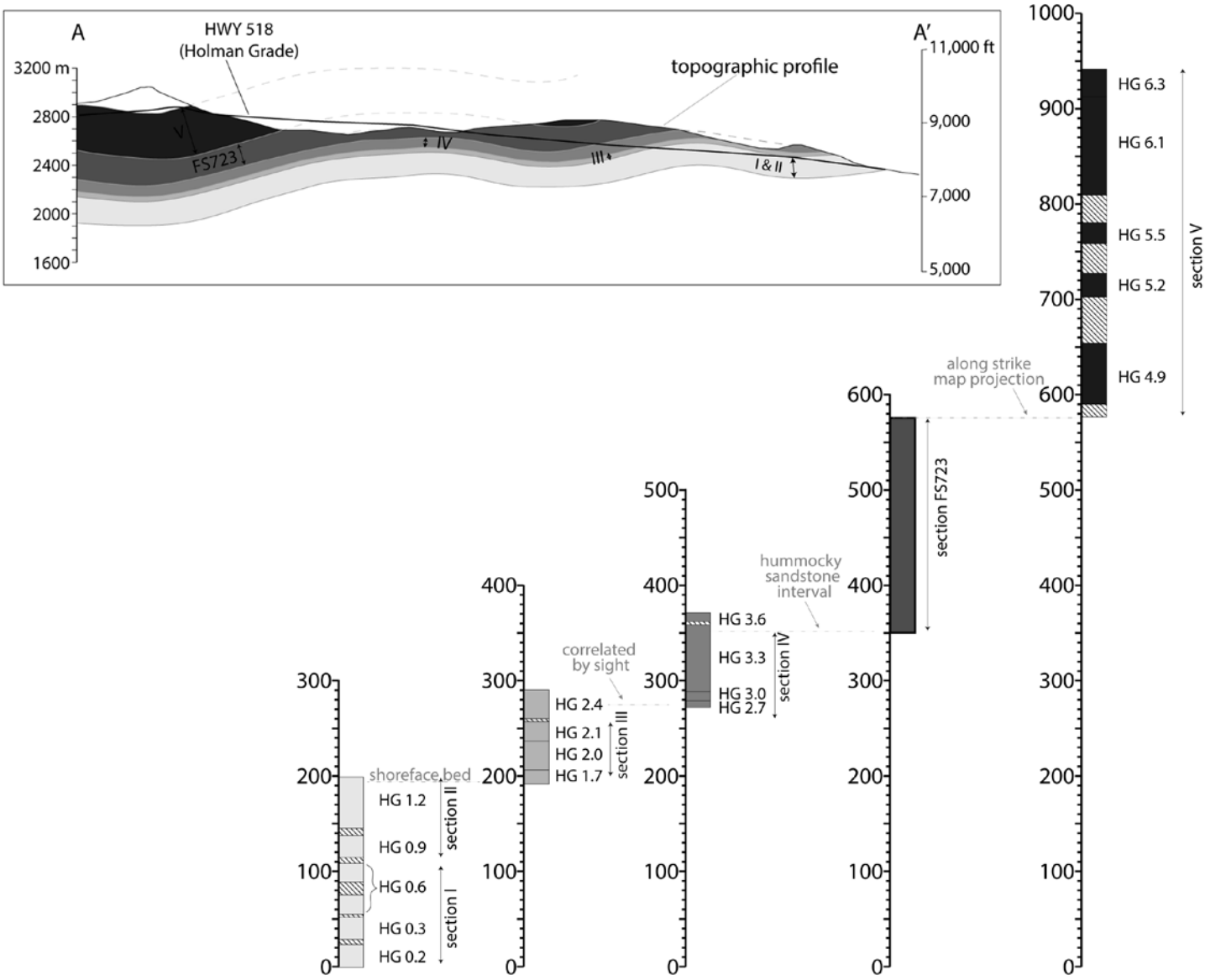

FIGURE 4. Key for demonstrating the construction of the composite section. Individual sections are noted by terminology HG plus mileage uphill from base of Holman Grade, see text for details. Location of cross-section A-A' and combined stratigraphic sections shown on Figure 3.

IMPLICATIONS FOR FILLING OF THE TAOS TROUGH

The Holman Grade section lies near the structural axis of the Taos trough as indicated by the thickest accumulation of Pennsylvanian strata within the basin (Fig. 1; Baltz and Myers, 1999). The entire stratigraphic thickness of the Pennsylvanian section here approaches 2500 m thick and ranges from Morrowan through Virgilian (Sutherland, 1963; Baltz and Myers, 1999). Desmoinesian conodonts recovered from the base (Latitude 36.0508°; Longitude -105.3922°) and top (Latitude 36.0720°; Longitude -105.4459°) of the composite section indicate that the Holman Grade section records an interval of basin fill approximately half-way through the Pennsylvanian history.

Soegaard (1990) proposed a flexural origin for the Taos trough where a tectonic load was emplaced via the steeply dipping Pecos-Picuris fault to the west (Fig. 1). A hallmark of flexural basin fill is a progressive filling of accommodation space from an underfilled basin to shallow marine or nonmarine deposition (e.g., DeCelles and Giles, 1996; Barbeau, 2003). Therefore, if the Taos trough formed in response to flexure, then the fill should represent a progressive filling of accommodation space or shallowing upward.

The facies present along the Holman Grade composite section are at odds with the flexural model. In the lower 490 m of the composite section, A-type cycles that shallow upward from offshore mudstone to non-marine facies occur eleven times. The nonmarine facies within these cycles indicate nearly complete filling of available accommodation space for each individual cycle. Thus, although A-type cycles demonstrate a shallowing upward package of strata, which by definition indicates a progressive filling of accommodation space, the eustatic and

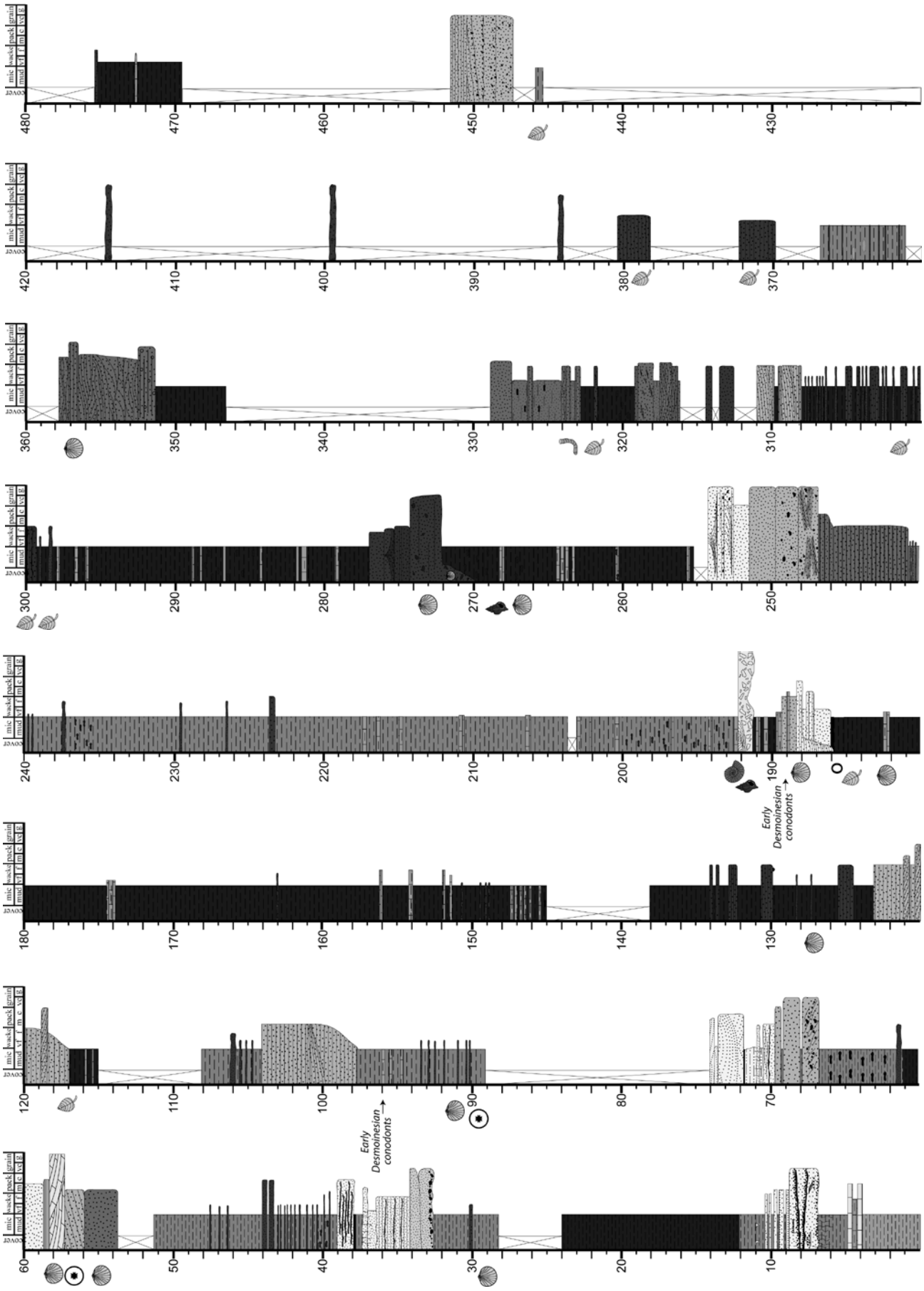

FIGURE 5. Composite stratigraphic section of Holman Grade. Symbology and lithology are keyed on Figure 6. Grain-size scale nomenclature: slt = silt, vf = very fine, f = fine, m = medium, c = coarse, vc = very coarse, g = granule, mic = micrite, wacke = wackestone, pack = packstone, grain = grainstone

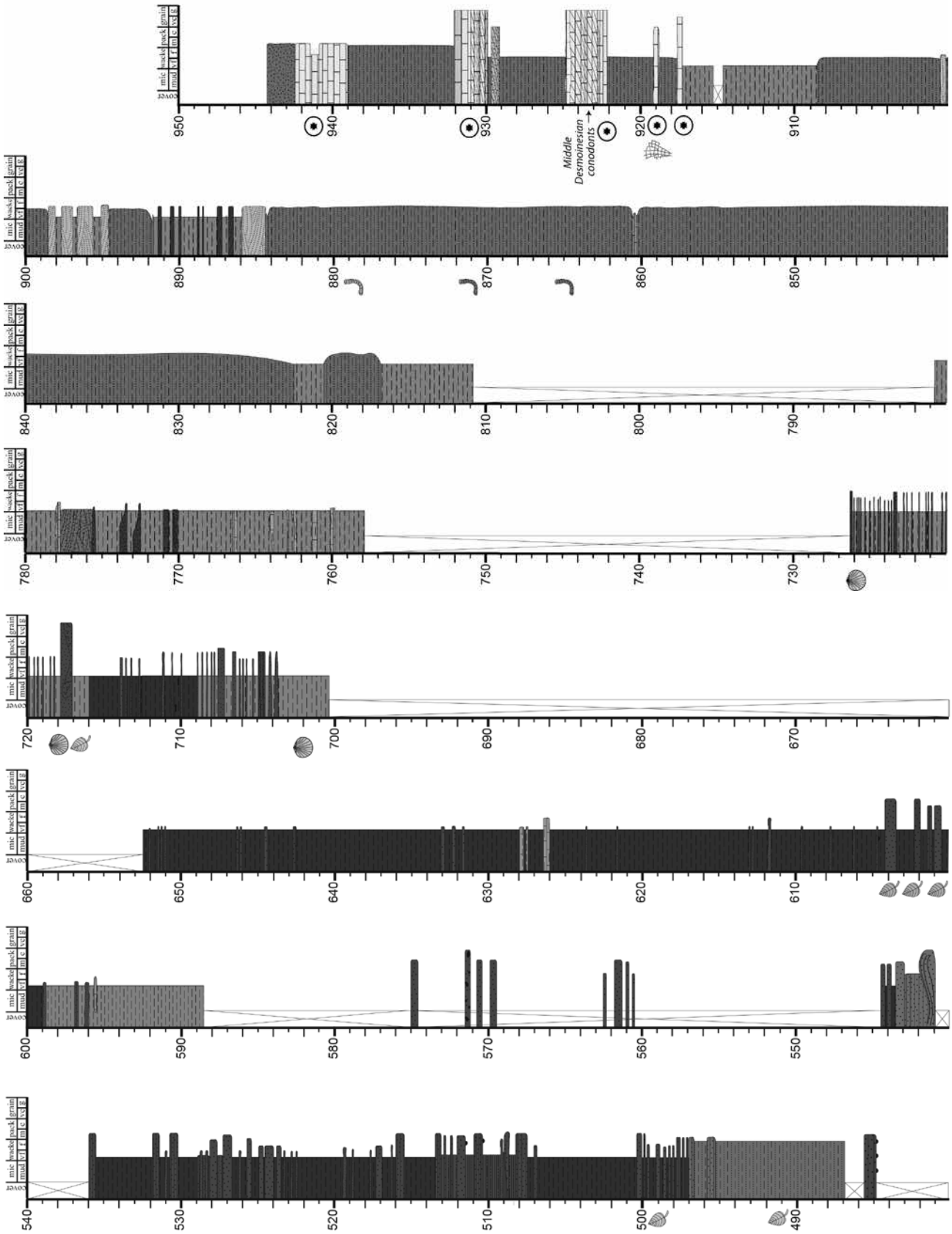

FIGURE 5. (Continued)

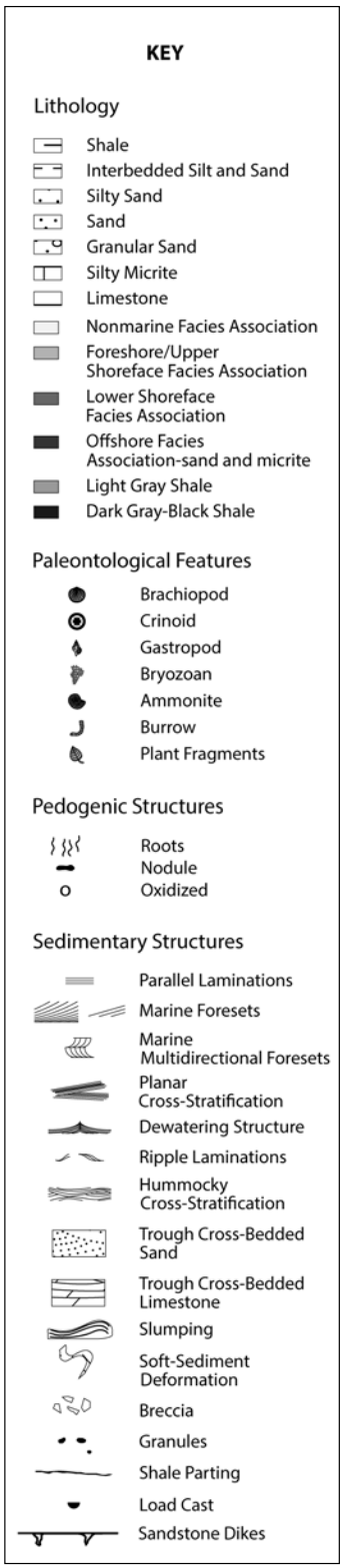

FIGURE 6. Key and legend to composite stratigraphic column (Figs. 5, 8).

FIGURE 7. Photographs of key facies exhibited in the Holman Grade composite section. A. Carbonaceous layer incised by fluvial channel. Note the base of the fluvial channel indicated by the white dashed line. Photograph illustrates strata at around 186 meters above base on figure 5. B. Cross-bedded sandstone with abundant crinoid allochems. Facies is inferred as upper shoreface sand body. Lens cap is approximately 5 cm diameter. C. Low-angle, planar-laminated sandstone inferred as upper shoreface sand body. Note height of foresets is equivalent to bed thickness which is approximately 120 cm. Photographs (B) and (C) represent strata around 55–57 m above base on Figure 5. D. Hummocky-cross stratification indicative of lower shoreface facies association. This facies also commonly forms B-type cycle tops. Lens cap for scale is approximately 5 cm in diameter. Photograph represents strata at around 355 meters above base on Figure 5. (See also Color Plate 15)

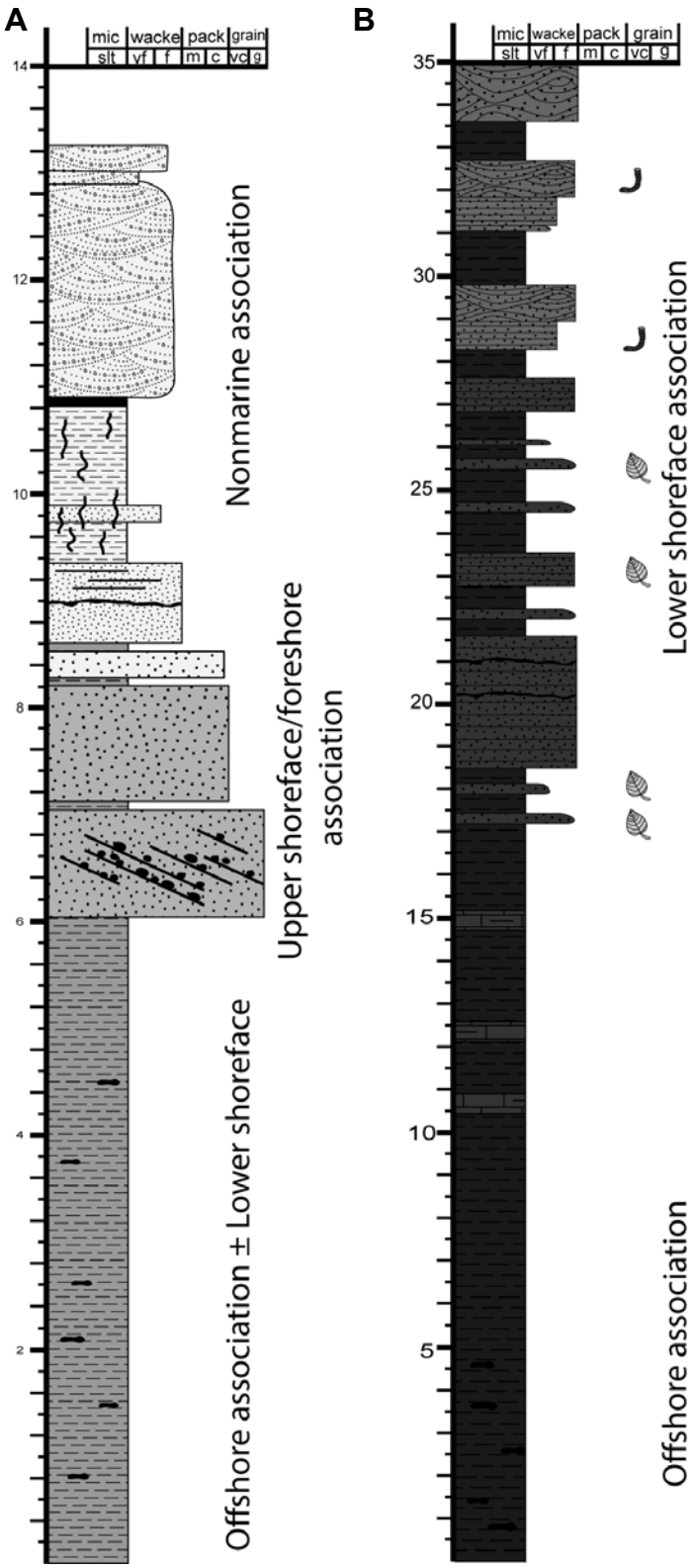

FIGURE 8. A. Schematic A-type cycle demonstrating shallowing upward succession from offshore mudstone to nonmarine fluvial facies. B. Schematic B-type cycle demonstrating shallowing upward from offshore mudstone to lower shoreface facies. Symbology keyed in Figure 6.

subsidence controls of accommodation never greatly outpaced sediment delivery. In contrast, the B-type cycles exhibit lower shoreface cycle tops indicating incomplete filling of accommodation space. Theoretically, a decrease in the rate of sediment delivery or a long-term rise in global sea level could allow for the incomplete filling of the B-type cycles. However, these controls are unlikely because local or regional mechanisms to reduce sediment supply are not readily identifiable and Desmoinesian records of relative sea level demonstrate that a continuous, long-term rise coeval to our section likely did not occur (Eros et al., 2012) and the high-frequency variations that are the hallmark of glacio-eustasy would give and take away accommodation. Alternatively, an uptick in the rate of subsidence could also account for the increase in accommodation space denoted by the unfilled B-type cycles. A backstripped subsidence history curve of the entire stratigraphic column within the Taos trough region appears to agree with an uptick in the rate of subsidence in the Desmoinesian (Watters, 2014) that is of much larger magnitude than Desmoinesian relative sea level rise observed in other basins (c.f. Eros et al., 2012.). Regardless of the control on accommodation space, the Holman Grade composite section demonstrates an increase in overall net accommodation upward in the section, as indicated by decreasing nonmarine and shallow marine deposits, whereas over the geologic life span of a flexural basin the opposite should be demonstrated (e.g., Barbeau, 2003). However, given that the Holman Grade section only records partial filling of the Taos trough, intermittent, thrust loading could result in upward deepening intervals (DeCelles and Giles, 1996). Regardless, the nonmarine facies present within the Taos trough axis have not been highlighted in previous work.

Similar to the character of fill within the Taos trough, reassessments of regional tectonic elements of the Taos trough are hard to reconcile with a flexural model. First, various workers demonstrate predominantly strike-slip history for the basin bounding Pecos-Picuris fault (e.g., Erslev et al., 2004; Wawrzyniec et al., 2007; Cather et al., 2011; Luther et al., 2012) indicating that the thrust mechanism to emplace the load for flexural response is lacking. Secondly, isopach map patterns and stratigraphic thinning relationships suggest the presence of intrabasinal structural highs (Fig. 1; Baltz and Myers, 1999) which if confirmed would indicate shortening in the center of the Soegaard (1990) flexural basin. At this time, we do not attempt to propose any new basin model for the Taos trough, but do note that any future structural models for the Taos trough would need to account for these three observations: (1) a middle Desmoinesian increase in subsidence; (2) a strike-slip basin bounding fault to the west; and (3) intrabasinal strain manifested as Precambrian-basement involved thrusts.

ACKNOWLEDGMENTS

Partial support was provided by SEPM student grant awarded to A.J. Watters. Reviews by S.M. Cather and R. Langford greatly improved the manuscript. We thank Texas Tech University students A. Saelens, B. Mathis and J. Lillegraven for field assistance. J.E. Barrick and C. Treat processed and identified the conodonts recovered in the section.

REFERENCES

Baltz, E. H., and Myers, D. A., 1984, Porvenir Formation (new name)—and other revisions of nomenclature of Mississippian, Pennsylvanian, and Lower Permian rocks, southeastern Sangre de Cristo Mountains, New Mexico: U.S. Geological Survey, Bulletin 1537-b, 39 p.

Baltz, E. H., and Myers, D. A., 1999, Stratigraphic framework of upper Paleozoic rocks, southeastern Sangre de Cristo Mountains, New Mexico, with a setion on speculations and implications for regional interpretation of Ancestral Rocky Mountains paleotectonics: New Mexico Bureau of Mines and Mineral Resources Memoir 48, 269 p.

Barbeau, D. L., 2003, A flexural model for the Paradox Basin: implications for the tectonics of the Ancestral Rocky Mountains: Basin Research, v. 15, no. 1, p. 97–115.

Cather, S. M., Read, A. S., Dunbar, N. W., Kues, B. S., Krainer, K., Lucas, S. G., & Kelley, S. A., 2011, Provenance evidence for major post–early Pennsylvanian dextral slip on the Picuris-Pecos fault, northern New Mexico: Geosphere, v. 7, no. 5, p. 1175–1193.

DeCelles, P.G. and Giles, K.A., 1996, Foreland basin systems: Basin Research, v. 8, p. 105–123.

Eros, J. M., Montañez, I. P., Osleger, D. A., Davydov, V. I., Nemyrovska, T. I., Poletaev, V. I., and Zhykalyak, M. V., 2012, Sequence stratigraphy and onlap history of the Donets Basin, Ukraine: insight into Carboniferous icehouse dynamics: Palaeogeography, Palaeoclimatology, Palaeoecology, v. 313, p. 1–25.

Erslev, E.A., Fankhauser, S.D., Heizler, M.T., Sanders, R.E., and Cather, S.M., 2004, Strike-slip tectonics and thermochronology of northern New Mexico: A field guide to critical exposures in the southern Sangre de Cristo Mountains; *in* Nelson, E.P., and Erslev, E.A., eds., Field trips in the southern Rocky Mountains: Geological Society of America Field Guide 5, p. 15–40.

Hoy, R. G., and Ridgway, K. D., 2002, Syndepositional thrust-related deformation and sedimentation in an Ancestral Rocky Mountains basin, Central Colorado trough, Colorado, USA: Geological Society of America Bulletin, v. 114, no. 7, p. 804–828.

Kluth, C. F., and Coney, P. J., 1981, Plate tectonics of the Ancestral Rocky Mountains: Geology, v. 9, p. 10–15.

Lindsey, D. A., Clark, R. F., Soulliere, S. J., 1986, Minturn and Sangre de Cristo Formations of Southern Colorado: A Prograding Fan Delta and Alluvial Fan Sequence Shed from the Ancestral Rocky Mountains: American Association of Petroleum Geologists Memoir 41, p. 541–561.

Luther, A., Axen, G., and Cather, S., 2012, Deciphering the early history of a multiply reactivated fault using strain analysis in an adjacent fold: Evidence for early brittle-plastic slip on the Picuris-Pecos fault, New Mexico, USA: Geosphere, v. 8, p. 703–715.

Miall, A. D., 1984, Deltas; *in* Walker, R.G., (ed.), Facies Models (Second edition): Geoscience Canada, Reprint Series 1, p. 105–118.

Reading, H. G., 1986, Sedimentary Environments and Facies. Blackwell Scientific, Oxford, London. 615 p.

Rygel, M. C., Fielding, C. R., Frank, T. D., and Birgenheier, L. P., 2008, The magnitude of Late Paleozoic glacioeustatic fluctuations: a synthesis: Journal of Sedimentary Research, v. 78, no. 8, p. 500–511.

Soegaard, K., 1990, Fan-delta and braid-delta systems in Pennsylvanian Sandia Formation, Taos Trough, northern New Mexico: Depositional and tectonic implications: Geological Society of America Bulletin, v. 102, p. 1325–1343.

Sutherland, P.K., 1963, Paleozoic rocks; *in* Miller, J.P., Montgomery, A., and Sutherland, P.K., eds., Geology of part of the southern Sangre de Cristo Mountains: New Mexico Bureau of Mines and Mineral Resources Memoir 11, p. 22–46.

Sweet, D. E., and Soreghan, G. S., 2010, Late Paleozoic tectonics and paleogeography of the ancestral Front Range: Structural, stratigraphic, and sedimentologic evidence from the Fountain Formation (Manitou Springs, Colorado): Geological Society of America Bulletin, v. 122, no. 3–4, 575–594.

Veevers, J. J., and Powell, C. M., 1987, Late Paleozoic glacial episodes in Gondwanaland reflected in transgressive-regressive depositional sequences in Euramerica: Geological Society of America Bulletin, v. 98, p. 475– 487.

Walker, R. G., 1984, Shelf and shallow marine sands; *in* Walker, R. G., ed., Facies models (second edition): Geoscience Canada, Reprint Series 1, p. 141–170.

Wanless, H. R., and Shepard, F. P., 1936, Sea level and climatic changes related to late Paleozoic cycles: Bulletin of the Geological Society of America, v. 47, p. 1,177–1,206

Watters, A.J., 2014, Middle Pennsylvanian Paleogeographic and Basin Analysis of the Taos trough, northern New Mexico. Unpublished MS thesis, Texas Tech University. 125 p.

Wawrzyniec, T.F., Ault, A.K., Geissman, J.W., Erslev, E.A., and Fankhauser, S.D., 2007, Paleomagnetic dating of fault slip in the southern Rocky Mountains, USA, and its importance to an integrated Laramide foreland strain field: Geosphere, v. 3, p. 16–25.

Yin, A., and Ingersoll, R. V., 1997, A Model for Evolution of Laramide Axial Basins in the Southern Rocky Mountains, U.S.A.: International Geology Review, v. 39, p. 1113–1123.